

FLOW REGIME IDENTIFICATION OF PARTICLES CONVEYING IN
PNEUMATIC PIPELINE USING ELECTRIC CHARGE TOMOGRAPHY AND
NEURAL NETWORK TECHNIQUES

HAKILO AHMED SABIT

A thesis submitted in fulfilment of the
requirements for the award of the degree of
Master of Engineering (Electrical)

Faculty of Electrical Engineering
Universiti Teknologi Malaysia

MARCH 2006

**Dedicated to my beloved mother Zahra Siyyo and to my brothers and sisters for
their support and prayers throughout**

ACKNOWLEDGEMENT

I would like to thank my supervisor Associate Professor Dr. Mohd Fua'ad bin Hj Rahmat for his support and encouragement during this project. At several stages in the course of this research project I benefited from his advice, particularly so when exploring new ideas. His positive outlook and confidence in my research inspired me and gave me confidence. His careful supervision and guidance contributed enormously to the successful completion of this thesis.

My sincere gratitude and thanks also goes to those who have contributed to the completion of this research directly or indirectly.

Finally I would like to express my sincere thanks and great appreciation to Universiti Teknologi Malaysia for the financial support of this project.

ABSTRACT

Solid particles flow in a pipeline is a common means of transportation in industries. Pharmaceutical industries, food stuff manufacturing industries, cement and chemical industries are some of the industries to exploit this transportation technique. For such industries, monitoring and controlling materials flow through the pipeline is essential to ensure plant efficiency and safety of the system. The pipeline transportation used in this research makes use of electrodynamic sensors which are charge to voltage converters. The process flow data is captured fitting an array of 16 such sensors around the circumference of the pipe to capture the inherent charge on the flowing solid materials. A high speed data acquisition card DAS1800HC is used to interface the sensors to a personal computer which processes the data using linear back projection algorithm (LBPA) and filtered back projection algorithm (FBPA). Data captured for this purpose is in the range of mass flow rates 26 g/s to 204 g/s. A Visual C++ programming language is used to develop an application program to compute the image reconstruction algorithms and display the tomograms which represent the concentration profiles at a measurement cross-section of the pipe. A neural network based flow regime identifier program is developed in Matlab environment. Baffles of different shapes are inserted to artificially create expected flow regimes and data captured in this way are used in training and evaluating the network's performance. This research has produced filtered back concentration profiles of each flow regimes owing to the technique of neural network method of flow regime identification.

ABSTRAK

Aliran partikel pepejal di dalam paip aliran adalah satu cara pengangkutan di dalam industri. Ini adalah kerana pengangkutan mampu mengelak pembaziran akibat tumpahan dan mengurangkan risiko di dalam mengendalikan bahan-bahan berbahaya. Industri farmaseutikal, industri penghasilan bahan makanan, simen, dan industri kimia adalah beberapa industri yang menggunakan kaedah pengangkutan ini. Untuk industri-industri seperti ini, pengawasan dan pengawalan bahan-bahan yang mengalir di dalam paip aliran adalah penting untuk memastikan kecekapan plant dan keselamatan sistem tersebut. Pengangkutan paip aliran yang digunakan di dalam kajian ini menggunakan penderia elektrodinamik yang merupakan penukar cas kepada voltan. Data aliran proses diambil daripada satu tatasusunan 16 penderia-penderia yang diletakkan di sekeliling paip untuk merakam sifat cas pada bahan-bahan pepejal yang mengalir. Satu kad perolehan data DAS18000HC berkelajuan tinggi telah digunakan sebagai pengantaramukaan diantara penderia-penderia kepada komputer peribadi yang memproses data yang sama menggunakan algoritma linear back projection (LBPA) dan algoritma filtered linear back projection (FBPA). Bahasa pengaturcaraan Visual C++ digunakan untuk membangun satu program aplikasi untuk menghitung algoritma-algoritma pembinaan semula imej dan memaparkan tomogram yang mewakili profil tumpuan pada satu pengukuran kawasan-keratan rentas paip. Satu rangkaian neural berasaskan program pengecam aliran rejim dibangunkan menggunakan persekitaran Matlab. Penghadang pelbagai bentuk telah dimasukkan untuk menghasilkan aliran rejim jangkaan dan data yang telah dirakam digunakan di dalam latihan dan penilaian prestasi rangkaian. Kajian ini telah menghasilkan pembaikan profil tumpuan hasil daripada pengecaman rejim aliran menggunakan teknik kaedah rangkaian neural.

CONTENTS

| CHAPTER | TITLE | PAGE |
|----------|---|-------|
| | TITLE | i |
| | DECLARATION | ii |
| | DEDICATION | iii |
| | ACKNOWLEDGEMENT | iv |
| | ABSTRACT | v |
| | ABSTRAK | vi |
| | CONTENTS | vii |
| | LIST OF TABLES | xi |
| | LIST OF FIGURES | xii |
| | LIST OF ABBREVIATIONS | xvii |
| | LIST OF APPENDICES | xviii |
| | | |
| 1 | INTRODUCTION | |
| | 1.1 An Overview of Process Tomography | 1 |
| | 1.2 Importance of Research | 3 |
| | 1.3 Problem Statement | 4 |
| | 1.4 Aims and Objectives of the Research | 4 |
| | 1.5 The Thesis Outline | 5 |
| | | |
| 2 | LITERATURE REVIEW | |
| | 2.1 Introduction | 7 |
| | 2.2 Tomography Sensors | 9 |

| | | |
|-------|---|----|
| 2.2.1 | Optical Tomography | 9 |
| 2.2.2 | Ultrasonic Tomography | 10 |
| 2.2.3 | Electrical Capacitance Tomography (ECT) | 12 |
| 2.2.4 | Electrical Impedance Tomography | 14 |
| 2.2.5 | Positron Emission Tomography | 15 |
| 2.2.6 | Electrodynamic Tomography | 17 |
| 2.3 | Flow Regime Identification Using Neural Networks | 19 |

3

TOMOGRAPHIC IMAGE RECONSTRUCTION MODEL

| | | |
|-------|--|----|
| 3.1 | Introduction | 21 |
| 3.2 | Particles Charging Mechanism in Pneumatic Conveying | 21 |
| 3.2.1 | Contact Electrification | 22 |
| 3.2.2 | Symmetric Charge Separation | 22 |
| 3.2.3 | Triboelectrification | 23 |
| 3.3 | Electrodynamic Sensors Operation | 23 |
| 3.4 | Tomographic Image Reconstruction for Electric Charge tomography | 24 |
| 3.4.1 | The Forward Problem | 24 |
| | 3.4.1.1 Sensitivity Map of Sensor 1 | 28 |
| | 3.4.1.2 Sensitivity Map of Sensor 2 | 31 |
| | 3.4.1.3 Sensitivity Map of Sensor 3 | 34 |
| | 3.4.1.4 Sensitivity Map of Sensors 4 to 16 | 36 |
| 3.4.2 | The Inverse Problem | 36 |
| | 3.4.2.1 Linear Back Projection Algorithm | 37 |
| | 3.4.2.2 Filtered Back Projection Algorithm | 38 |

| | | |
|----------|---|-----|
| 4 | ARTIFICIAL NEURAL NETWORKS | |
| 4.1 | Introduction | 44 |
| 4.2 | Back-Propagation network for Flow Regime Identification | 50 |
| 5 | DESIGN OF THE MEASUREMENT SYSTEM | |
| 5.1 | Introduction | 60 |
| 5.2 | The Gravity Flow Rig | 60 |
| 5.3 | Measurement System | 63 |
| 5.3.1 | Electrodynamic Sensor | 64 |
| 5.3.2 | The Data Acquisition System | 68 |
| 5.3.3 | Data Storage and Processing | 70 |
| 5.4 | Application Program and Image Display | 71 |
| 5.5 | Flow Regimes | 75 |
| 6 | RESULTS | |
| 6.1 | Introduction | 84 |
| 6.2 | Experimental Results of Sensors Response | 85 |
| 6.3 | Averaged Output of the Sensors | 87 |
| 6.4 | Comparison of Measured and Predicted Output | 92 |
| 6.4.1 | Full Flow | 92 |
| 6.4.2 | Three-quarter Flow | 98 |
| 6.4.3 | Half Flow | 104 |
| 6.4.4 | Quarter Flow | 109 |
| 6.5 | Flow Regime Identification from Measured Data | 114 |
| 6.5.1 | Training Patterns | 115 |
| 6.5.2 | Test Patterns | 120 |
| 6.6 | Concentration Profiles | 122 |
| 6.6.1 | Full Flow | 122 |
| 6.6.2 | Three-quarter Flow | 126 |
| 6.6.3 | Half Flow | 129 |

| | | |
|-------|--------------------------------------|-----|
| 6.6.4 | Quarter Flow | 133 |
| 6.6.5 | Discussions of Concentration Profile | 137 |
| | Results | |

7**CONCLUSION AND SUGGESTIONS FOR FUTURE
WORK**

| | | |
|-----|-------------------------------|-----|
| 7.1 | Conclusion | 140 |
| 7.2 | Contributions of the Research | 141 |
| 7.3 | Suggestions for Further Work | 142 |

| | | |
|--|-------------------|-----|
| | REFERENCES | 144 |
|--|-------------------|-----|

| | | |
|--|-------------------|-----|
| | APPENDICES | 148 |
|--|-------------------|-----|

LIST OF TABLES

| TABLES | TITLE | PAGE |
|---------------|---|-------------|
| 3.1 | Procedure for obtaining the sensitivity maps of sensors 4 to 16 | 36 |
| 4.1 | Flow regime specific target vectors | 56 |
| 5.1 | Relative output of each sensor for full flow case | 77 |
| 5.2 | Relative output of each sensor for three-quarter flow case | 79 |
| 5.3 | Relative output of each sensor for half flow case | 81 |
| 5.4 | Relative output of each sensor for quarter flow case | 83 |
| 6.1 | Measured-to-predicted outputs difference for full flow case | 97 |
| 6.2 | Measured-to-predicted outputs difference for three-quarter flow case | 102 |
| 6.3 | Measured-to-predicted outputs difference for half flow case | 108 |
| 6.4 | Measured-to-predicted outputs difference for quarter flow case | 113 |
| 6.5 | Sample training pattern data | 115 |
| 6.6 | Flow regimes codes | 117 |
| 6.7 | Successful identification of flow regimes | 121 |
| 6.8 | The network outputs for 10 data sets | 121 |
| 6.9 | Sum of pixels values for linear back projection | 137 |
| 6.10 | Sum of pixels values for filtered back projection | 138 |

LIST OF FIGURES

| FIGURES | TITLE | PAGE |
|----------------|---|-------------|
| 1.1 | An overview of a process tomography system | 2 |
| 2.1 | Process tomography system | 8 |
| 3.1 | An 11x11 rectangular array of 121 pixels with sensors positions | 25 |
| 3.2 | The pipe co-ordinate model | 26 |
| 3.3 | Pixels identity | 27 |
| 3.4 | The sensitivity model | 28 |
| 3.5 | Sensitivity map of sensor 1 | 30 |
| 3.6 | 3D sensitivity map of sensor 1 | 31 |
| 3.7 | Sensitivity map of sensor 2 | 33 |
| 3.8 | 3D sensitivity map of sensor 2 | 33 |
| 3.9 | Sensitivity map of sensor 3 | 35 |
| 3.10 | 3D sensitivity map of sensor 3 | 35 |
| 3.11 | Concentration matrix | 37 |
| 3.12 | Theoretical concentration matrix tomogram | 38 |
| 3.13 | Filter mask for full flow in matrix format | 39 |
| 3.14 | Filter mask for full flow in 3D format | 40 |
| 3.15 | Theoretical concentration profile using filtered back-projection | 41 |
| 3.16 | Theoretical concentration profile using filtered back-projection algorithm in 3D format | 41 |
| 3.17 | Three-quarter flow filter mask | 42 |
| 3.18 | Half flow filter mask | 42 |
| 3.19 | Quarter flow filter mask | 43 |
| 4.1 | A biological neuron | 46 |
| 4.2 | An artificial neuron | 46 |
| 4.3 | Feedforward artificial neural network | 47 |

| | | |
|------|---|-----|
| 4.4 | feedback artificial neural network | 48 |
| 4.5 | Feedforward back propagation network | 57 |
| 4.6 | Log-sigmoid function plot | 58 |
| 5.1 | The laboratory gravity flow rig diagram | 62 |
| 5.2 | Calibration curve of the gravity flow rig | 63 |
| 5.3 | Photo of an electrodynamic sensor | 66 |
| 5.4 | Block diagram of electrical charge sensor | 67 |
| 5.5 | Electrode Receptacle | 68 |
| 5.6 | Diagram of sensor array connection to the PC | 70 |
| 5.7 | Block diagram of application program tasks | 73 |
| 5.8 | The main GUI of the application program | 74 |
| 5.9 | Side and top view of full flow baffle | 76 |
| 5.10 | Predicted relative voltage output for full flow | 76 |
| 5.11 | Side and top view of three-quarter flow baffle | 78 |
| 5.12 | Predicted relative voltage output for three-quarter flow | 78 |
| 5.13 | Side and top view of half flow baffle | 80 |
| 5.14 | Predicted relative voltage output for half flow | 80 |
| 5.15 | Side and top view of quarter flow baffle | 82 |
| 5.16 | Predicted relative voltage output for quarter flow | 82 |
| 6.1 | Output of the sensors 1 to 16 at no flow condition | 85 |
| 6.2 | Average output of the 16 sensors at flow rates of 0 to 204 g/s | 88 |
| 6.3 | Measured and predicted outputs compared for full flow | 93 |
| 6.4 | Sum of measured sensors output and predicted output along with their linear regression lines plotted against mass flow rate for full flow case | 97 |
| 6.5 | Measured and predicted outputs compared for thee-quarter flow | 98 |
| 6.6 | Sum of measured sensors output and predicted output along with their linear regression lines plotted against mass flow rate for three-quarter flow case | 103 |
| 6.7 | Measured and predicted outputs compared for half flow | 104 |
| 6.8 | Sum of measured sensors output and predicted output along with their linear regression lines plotted against mass flow rate for half flow case | 108 |
| 6.9 | Measured and predicted outputs compared for quarter flow | 109 |

| | | |
|------|---|-----|
| 6.10 | Sum of measured sensors output and predicted output along with their linear regression lines plotted against mass flow rate for quarter flow case | 114 |
| 6.11 | Training patterns at lower flow rates | 116 |
| 6.12 | Training patterns at higher flow rates | 117 |
| 6.13 | The performance curve of trainlm algorithm | 118 |
| 6.14 | The performance curve of traingda algorithm | 118 |
| 6.15 | The performance curve of traingdx algorithm | 119 |
| 6.16 | The performance curve of trainrp algorithm | 119 |
| 6.17 | Concentration profiles for full flow at 45 g/s (LBPA) in numerical and 2D image format | 122 |
| 6.18 | Concentration profiles for full flow at 45 g/s (FBPA) in numerical and 2D image format | 123 |
| 6.19 | Concentration profiles for full flow at 85 g/s (LBPA) in numerical and 2D image format | 123 |
| 6.20 | Concentration profiles for full flow at 85 g/s (FBPA) in numerical and 2D image format | 123 |
| 6.21 | Concentration profiles for full flow at 125 g/s (LBPA) in numerical and 2D image format | 124 |
| 6.22 | Concentration profiles for full flow at 125 g/s (FBPA) in numerical and 2D image format | 124 |
| 6.23 | Concentration profiles for full flow at 165 g/s (LBPA) in numerical and 2D image format | 124 |
| 6.24 | Concentration profiles for full flow at 165 g/s (FBPA) in numerical and 2D image format | 125 |
| 6.25 | Concentration profiles for full flow at 204 g/s (LBPA) in numerical and 2D image format | 125 |
| 6.26 | Concentration profiles for full flow at 204 g/s (FBPA) in numerical and 2D image format | 125 |
| 6.27 | Concentration profiles for three-quarter flow at 45 g/s (LBPA) in numerical and 2D image format | 126 |
| 6.28 | Concentration profiles for three-quarter flow at 45 g/s (FBPA) in numerical and 2D image format | 126 |

| | | |
|------|---|-----|
| 6.29 | Concentration profiles for three-quarter flow at 85 g/s (LBPA) in numerical and 2D image format | 127 |
| 6.30 | Concentration profiles for three-quarter flow at 85 g/s (FBPA) in numerical and 2D image format | 127 |
| 6.31 | Concentration profiles for three-quarter flow at 125 g/s (LBPA) in numerical and 2D image format | 127 |
| 6.32 | Concentration profiles for three-quarter flow at 125 g/s (FBPA) in numerical and 2D image format | 128 |
| 6.33 | Concentration profiles for three-quarter flow at 165 g/s (LBPA) in numerical and 2D image format | 128 |
| 6.34 | Concentration profiles for three-quarter flow at 165 g/s (FBPA) in numerical and 2D image format | 128 |
| 6.35 | Concentration profiles for three-quarter flow at 204 g/s (LBPA) in numerical and 2D image format | 129 |
| 6.36 | Concentration profiles for three-quarter flow at 204 g/s (FBPA) in numerical and 2D image format | 129 |
| 6.37 | Concentration profiles for half flow at 45 g/s (LBPA) in numerical and 2D image format | 130 |
| 6.38 | Concentration profiles for half flow at 45 g/s (FBPA) in numerical and 2D image format | 130 |
| 6.39 | Concentration profiles for half flow at 85 g/s (LBPA) in numerical and 2D image format | 130 |
| 6.40 | Concentration profiles for half flow at 85 g/s (FBPA) in numerical and 2D image format | 131 |
| 6.41 | Concentration profiles for half flow at 125 g/s (LBPA) in numerical and 2D image format | 131 |
| 6.42 | Concentration profiles for half flow at 125 g/s (FBPA) in numerical and 2D image format | 131 |
| 6.43 | Concentration profiles for half flow at 165 g/s (LBPA) in numerical and 2D image format | 132 |
| 6.44 | Concentration profiles for half flow at 165 g/s (FBPA) in numerical and 2D image format | 132 |
| 6.45 | Concentration profiles for half flow at 204 g/s (LBPA) in numerical and 2D image format | 132 |

| | | |
|------|---|-----|
| 6.46 | Concentration profiles for half flow at 204 g/s (FBPA) in numerical and 2D image format | 133 |
| 6.47 | Concentration profiles for quarter flow at 45 g/s (LBPA) in numerical and 2D image format | 133 |
| 6.48 | Concentration profiles for quarter flow at 45 g/s (FBPA) in numerical and 2D image format | 134 |
| 6.49 | Concentration profiles for quarter flow at 85 g/s (LBPA) in numerical and 2D image format | 134 |
| 6.50 | Concentration profiles for quarter flow at 85 g/s (FBPA) in numerical and 2D image format | 134 |
| 6.51 | Concentration profiles for quarter flow at 125 g/s (LBPA) in numerical and 2D image format | 135 |
| 6.52 | Concentration profiles for quarter flow at 125 g/s (FBPA) in numerical and 2D image format | 135 |
| 6.53 | Concentration profiles for quarter flow at 165 g/s (LBPA) in numerical and 2D image format | 135 |
| 6.54 | Concentration profiles for quarter flow at 165 g/s (FBPA) in numerical and 2D image format | 136 |
| 6.55 | Concentration profiles for quarter flow at 204 g/s (LBPA) in numerical and 2D image format | 136 |
| 6.56 | Concentration profiles for quarter flow at 204 g/s (FBPA) in numerical and 2D image format | 136 |
| 6.57 | Sum of pixels values versus flow rate for linear back projection | 138 |
| 6.58 | Sum of pixels values versus flow rate for filtered back projection | 139 |

LIST OF ABBREVIATIONS

| | |
|--------|------------------------------------|
| 2D | Two dimensions |
| 3D | Three dimensions |
| ACF | Attenuation correction factor |
| ANN | Artificial neural network |
| BP | Back-Propagation |
| DAS | Data acquisition system |
| ECT | Electrical capacitance tomography |
| EIT | Electrical impedance tomography |
| FBP | Filtered back projection |
| FBPA | Filtered back projection algorithm |
| GUI | Graphical user interface |
| LBP | Linear back projection |
| LBPA | Linear back propagation algorithm |
| Logsig | Logarithmic sigmoid |
| LOR | Line of response |
| PC | Personal computer |
| PET | Positron emission tomography |

LIST OF APPENDICES

| APPENDIX | TITLE | PAGE |
|-----------------|--|-------------|
| A | Flow regime identifier program source code in Matlab environment | 148 |
| B | Electrodynamic sensor circuit | 151 |
| C | Application program (Visual C++) source codes | 152 |
| D | Application program users manual | 179 |
| E | The noise signal of the 16 electrodynamic sensors at no flow condition | 183 |
| F | Numerical and color 2D image concentration profiles of full flow | 189 |
| G | Numerical and color 2D image concentration profiles of three-quarter flow | 194 |
| H | Numerical and color 2D image concentration profiles of half flow | 199 |
| I | Numerical and color 2D image concentration profiles of quarter flow | 204 |

CHAPTER 1

INTRODUCTION

1.1 An Overview of Process Tomography

Tomography is a Greek term which stands for cross-sectional picture. It involves obtaining cross-sectional images of a body or a process. One of the earliest applications of tomography is in the field of medicine where a particular plane in a human body is imaged using this technique for diagnosis purposes.

The application of tomographic methods in industries for the purpose of better process control, optimization and efficient production is known as process tomography. Though the application of modern tomographic techniques only dates back few decades, process tomography has found applications in various industries such as chemical, oil, gas, food processing, biomedical, pharmaceuticals and plastic products manufacturing industries.

The use of process tomography is not limited to only obtaining cross-sectional image of processes. It can also be used to obtain velocity profiles and mass-flows rate or volume flow rates. Depending on the sensing mechanism used process tomography can be used in processes involving solids, liquids, gases and any of their mixtures.

Electrical tomography is one of the most investigated fields in process tomography. It is non-invasive, cost effective, safe and easy to implement technique. Electrical charge tomography is a system used in imaging particulate

flow in pipelines using electrodynamic sensors (charge-to-voltage transducers). It's a passive transducer where the field is generated by the flowing solid particles.

The motivation for using electrodynamic sensors as the sensing device in tomography arises from the fact that many flowing materials pick up charge during transportation, primarily by virtue of friction of fine particles amongst themselves and abrasion on the walls of the conveyor (Cross, 1987).

Based on the above fact electrodynamic sensors can be used to measure the charge on the flowing materials and convert it to voltage so that spatial information of the flowing material in the cross-section of the conveyor could be obtained.

In this research a circular array of 16 electrodynamic sensors is fitted to the circumference of the conveying pipe to detect the inherent charge on the flowing particles. Each electrodynamic sensor detects the charge on the particles flowing in its sensing zone and transforms the sensed charge in the form of corresponding electrical signal (voltage) level. In the same manner all the 16 electrodynamic sensors yield the level of sensed signal. The signals from the array of electrodynamic sensors are conditioned and amplified to a level suitable for data acquisition system. The data acquisition system then converts the simultaneously captured data to a digital format. The data acquisition system is used as an interface between the sensors and the personal computer (PC) used in data storage and processing. These data are then manipulated using image reconstruction algorithms to obtain tomographic images in an offline method. The flow data are also used in obtaining flow rates, concentration, size and phase distribution. An overview of process tomography block diagram is shown in Figure 1.1.

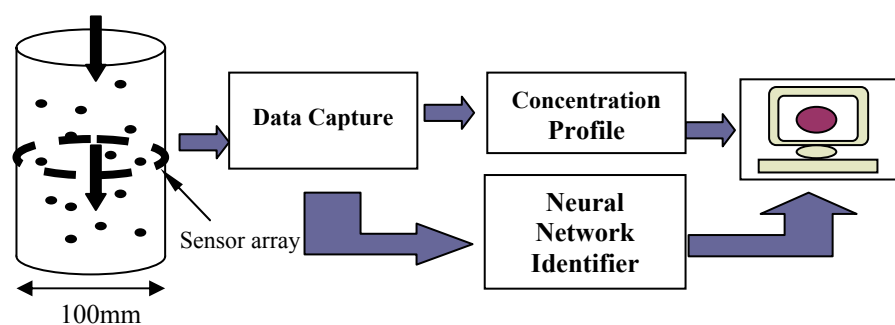


Figure 1.1: An overview of a Process Tomography System

1.2 Importance of Research

Particulate material handling by pneumatic conveying is extensively used in many industries such as food stuff processing, pharmaceutical, plastic product manufacturing, textiles, paper manufacturing, solids waste treatment and others.

The importance of research into pneumatic conveying can be viewed from the following points.

1. Safety problems: hazardous chemical transportation by formal means (road, ships and rail) are risky and could endanger the environment through leakages.
2. Waste reduction: spillage in pneumatic conveying can easily be detected and taken care of before the waste is significantly large.
3. Pollution control: many factories release waste into the atmosphere via chimneys which could be harmful particulate matters for the environment. This situation can be monitored through electrical charge tomography techniques.
4. Explosion hazard: the accumulation of static charge on solid materials being conveyed in industries could reach a level that can cause fire. This situation can also be monitored through electric charge tomography technique.
5. Blockage of conveyor: unexpected foreign material presence within the conveyor can affect efficiency of transportation which may be detected and avoided in time.

1.3 Problem Statement

Electrical charge tomography is the most suitable technique for imaging of solids flow in pneumatic pipelines whenever the solids phase density is low. There are a number of works done in applying electrodynamic tomography system to produce tomographic images of solid particles flow in pneumatic pipelines using tomographic image reconstruction algorithms. However, electrodynamic sensors being near sensor dominant has affected the accuracy of the resulting tomograms calculated using the linear back projection image reconstruction algorithm (section 3.4.2.1 of chapter 3).

In order to rectify this drawback of electrodynamic sensors, a second image reconstruction algorithm called filtered back projection algorithm (section 3.4.2.2, of chapter 3) is introduced. This algorithm combines filter masks to compensate for the lost signal strength for units further away from the sensors. However a situation arises when the conveyed flow regime is different from full flow (uniform particles distribution).

The filter masks for different flow regimes are different and therefore prior knowledge of flow regime being conveyed is necessary in order to determine the right filter mask. This research investigates artificial neural networks technique of flow regimes identification from row sensors output data so that tomograms of better accuracy can be obtained.

1.4 Aims and Objectives of the Research

The aim of this research is to detect the inherent charge on dry moving solid particles using electrodynamic sensors and to provide data of concentration profiles to verify the existing mathematical models using neural network as a tool.

The specific objectives of the research are to:

1. Become familiar with process tomography and artificial neural network concepts.
2. Design a measurement section for a pneumatic conveyor.
3. Test the complete measurement section on the gravity conveyor.
4. Measure peripheral pneumatically conveyed particles concentration profiles.
5. Simulate four different flow regimes by inserting baffles to obtain training data for a neural network to identify flow regimes.
6. Generate concentration profiles over the cross-section of the conveyor.
7. Identify the flow regimes in a pneumatic conveyor using artificial neural network technique.
8. Make suggestions for future works based on the acquired results.

1.5 The Thesis Outline

Chapter 1 presents general introduction to tomography and process tomography.

Chapter 2 presents an overview of different sensing mechanisms suitable for measurement of pneumatically conveyed particles. An electrodynamic system is proposed and artificial neural network based flow regimes identification is outlined.

Chapter 3 describes several mechanisms by which solid particles conveying in pneumatic pipeline acquire charge. The working principles of electrodynamic sensors are reviewed and the sensitivity models of electrodynamic sensors are developed.

Chapter 4 presents the principles of artificial neural networks and proposes the use of back-propagation network for flow regime identification. Weights and biases adaptation equations for the back-propagation network are derived.

Chapter 5 discusses the overall electrodynamic tomography measurement system. The configuration of electrodynamic sensors array, the gravity flow rig, data acquisition and storage, the artificial flow baffles and application development are described.

Chapter 6 presents the results using electrodynamic sensors, the performance of neural network in identifying flow regimes, concentration profiles and tomographic images.

Chapter 7 presents the overall conclusion and suggestion for future research.

- Different solid materials and different particle size materials should be used to determine the suitability of the measurement system for different materials and sizes.
- Calculating concentration profiles directly from sensors output by using neural network techniques (without using image reconstruction algorithms) should be considered.

REFERENCES

1. Azrita, A. (2002). "Mass Flow Visualization of Solid particles in Pneumatic Pipelines using Electrodynamic Tomography System", Universiti Teknologi Malaysia: M.E. Thesis.
2. Beck, M.S., and Plaskowski, A. (1987). "Cross Correlation Flowmeters-Their Design and Application". Bristol, England: Adam Hilger.
3. Beck, M.S., and Williams, R.A. (1996). "Process tomography: a European innovation and its applications". Meas. Sci. Technol Journal. Vol.7.P.215-224.
4. Bidin, A.R. (1993). "Electrodynamic Sensors and Neural Networks for Electrical Charge Tomography". Sheffield Hallam University: Ph.D Thesis.
5. Brown, G.J., Reilly, and D., Mills, D. (1996). "Development of an ultrasonic tomography system for application in pneumatic conveying". Meas. Sci. Technol Journal. Vol.7.P.396-405.
6. Champion, C., and Loirec, C. Le. (2006). "Positron follow-up in liquid water: I. A new monte carlo track-structure code". Phys. Med. Biol. Journal. Vol.51.pp.1707-1723.
7. Fang, W. (2004). "A nonlinear image reconstruction algorithm for electrical capacitance tomography". Meas. Sci. Tehnol Journal. Vol.15.pp.2124-2132.
8. Gajewski, J.B. (1996). "Electrostatic, inductive ring probe bandwidth", Meas. Sci. Technol Journal. Vol.7.pp.1766-1775.
9. Gao, N., Zhu, S.A., and He, B. (2005). "Estimation of electrical conductivity distribution within the human head from magnetic flux density measurement". Phys. Med. Biol. Journal. Vol.50.pp.2675-2687.

10. Green, R.G., Rahmat, M.F., Evans, K., Goude, A., Henry, M. and Stone, J.A.R. (1997). "Concentration profiles of dry powders in a gravity conveyor using an electrodynamic tomography system", *Meas. Sci. Technol Journal*. Vol.8.pp.192-197.
11. Gregory, I.A. (1987). "Shot velocity measurement using electrodynamic transducers". University of Manchester Institute of Science and Technology: Ph.D Thesis.
12. Guerrero, T., Castillo, R., Sanders, K., Price, R., Komaki, R., and Cody, D. (2006). "Novel method to calculate pulmonary compliance images in rodents from computed tomography acquired at constant pressures". *Phys. Med. Biol. Journal*. Vol.51.pp.1101-1112.
13. Hauptmann, P., Hoppe, and N., Puttmer, A. (2002). "Application of ultrasonic sensors in the process industry". *Meas. Sci. Technol Journal*. Vol.13.pp.R73-R83.
14. Hezri, M.F.R. (2002). "Real time velocity profile generation of powders conveying using electrical charge tomography". Universiti Teknologi Malaysia: M.E. Thesis.
15. Hoyle, B.S. (1996). "Process tomography using ultrasonic sensors". *Meas. Sci. Technol Journal*. Vol.7.pp.272-280.
16. Koksai, A., and Eyuboglu, B.M. (1995). "Determination of optimum injected current patterns in electrical impedance tomography". *Physiol. Meas. Journal*. Vol.16.pp.A99-A109.
17. Mustafa, K., Leblebicioglu, K., and Ider, Y.Z. (1994). "A fast image reconstruction algorithm for electrical impedance tomography". *Physiol. Meas. Journal*. Vol.15.pp.A115-A124.

18. Otten, D.M., and Rubinsky, B. (2005). "Front-tracking image reconstruction algorithm for EIT-monitored cryosurgery using the boundary element method". *Physiol. Meas. Journal*. Vol.26.pp.503-516.
19. Parker, D.J., and McNeil, P.A. (1996). "Positron emission tomography for process applications". *Meas. Sci. Technol Journal*. Vol.7.pp.287-296.
20. Rahmat, M.F. (1996). "Instrumentation of Particle Conveying Using Electrical Charge Tomography". Sheffield Hallam University: Ph.D Thesis.
21. Reinecke, N. and Mewes, D. (1996). "Recent developments and industrial/research applications of capacitance tomography". *Meas. Sci. Technol Journal*. Vol.7.pp.233-246.
22. Saleh, J.M., Hoyle, B.S., Podd, F.J.W, and Spink, D.M. (2001). "Direct flow process estimations from tomographic data using artificial neural systems". *Proceedings of 2nd world congress on Industrial process tomography*. (Hannover, Germany, 2001) pp751-8.
23. Sallehuddin, I. (2000). "Measurement of gas bubbles in a vertical water column using optical tomography". Sheffield Hallam University: Ph.D Thesis.
24. Shackleton, M.E. (1982). "Electrodynamic transducers for gas/solids flow measurement". University of Bradford: M.Phil Thesis.
25. Vandenberghe, S., Daube-witherspoon, M.E., Lewit, R.M., and Karp, J.S. (2006). "Fast reconstruction of 3D time-of-flight PET data by axial rebinning and transverse mashing". *Phys. Med. Biol. Journal*. Vol.51.pp.1603-1621.
26. Waristo, W. and Fan, L-S. (2001). "Neural network bases multi-criterion optimization image reconstruction technique for imaging two- and three-

- phase flow systems using electrical capacitance tomography”. *Meas. Sci. Technol Journal*. Vol.12.pp.2198-2210.
27. White, R.B. (2002). “Using electrical capacitance tomography to monitor gas voids in a packed bed of solids”. *Meas. Sci. Technol Journal*. Vol.13.pp.1842-1847.
28. Yan, H., Liu, Y.H., and Liu, C.T. (2004). “Identification of flow regimes using back-propagation networks trained on simulated data based on a capacitance tomography sensor”. *Meas. Sci. Technol Journal*. Vol.15..432-pp436.
29. Yan, Y. (1996). “Mass flow measurement of bulk solids in pneumatic pipelines”. *Meas. Sci. Technol Journal*. Vol.7.pp.1687-1706.
30. Yang, W.Q. and Peng, L. (2003). “Image reconstruction algorithms for electrical capacitance tomography”. *Meas. Sci. Technol Journal*. Vol.14.pp.R1-R13.
31. Yu, S.K., and Nahmias, C. (1996). “Segmented attenuation correction using artificial neural networks in positron tomography”. *Phys. Med. Biol. Journal*. Vol.41.pp.2189-2206.